J. Nanosci. Tech. - Volume 3 Issue 4 (2017) 299–303

Share Your Innovations through JACS Directory

Journal of Nanoscience and Technology

Visit Journal at http://www.jacsdirectory.com/jnst

ISSN: 2455-0191

Enhanced Photocatalytic Activity of Undoped ZnO on Methtyl Orange in Comparison with Doped ZnO and Theoretical Insight on Its Properties

V. Nirmala[1], S. Kalaiarasi[2], R. Rajakumari[1,*]

[1]*PG and Research Department of Physics, Queen Mary's College (Autonomous), Chennai – 600 004, Tamil Nadu, India.*
[2]*Department of Physics, Jaya College of Arts and Science, Chennai – 602 024, Tamil Nadu, India.*

ARTICLE DETAILS

Article history:
Received 03 November 2017
Accepted 29 November 2017
Available online 10 December 2017

Keywords:
Photocatalytic Study
Methyl Orange
Surface Defects
Ferromagnetic Interaction

ABSTRACT

This paper deals with the degradation effect of undoped and doped ZnO as photocatalysts on methyl orange (MO). The undoped and doped ZnO photocatalysts were synthesized by wet chemical method. The photocatalytic study of the synthesized samples was carried out under UV light in the short wavelength range of 254 nm with UV- absorption analysis. It was observed from the UV absorption analysis that undoped ZnO has pronounced effect in the degradation of MO in comparison with Ti^{4+}, Cu^{2+}, Mn^{2+} ion doped ZnO. This result suggests that, the larger band gap of undoped ZnO (3.37 eV for bulk ZnO), would have promoted the photocatalysis upon UV illumination with MO. In addition to this, surface defects would have played a role in the degradation of MO in this metal oxide semiconductor. The vibrating sample magnetometer study of transition metal ion doped ZnO exhibited ferromagnetic interaction at room temperature. It was also observed from the present study that the wet chemical method of synthesis of ZnO and ZnO based compounds has the advantage of producing nano sized crystallized powder of high purity at low temperature. Theoretical investigation on the properties of undoped and doped ZnO has also been carried out. From theoretical calculations, it is observed that undoped Zn_6O_6 cluster is kinetically stable when compared with transition metal ion doped Zn_6O_6 cluster.

1. Introduction

Photocatalytic activity is an ability of some nano materials (e.g. TiO_2) to speed up a certain reaction ("photoreaction") as a catalyst in combination with light (sunlight, ultraviolet light). In photogenerated catalysis, the photocatalytic activity depends on the ability of the catalyst to create electron–hole pairs, which generate free radicals (e.g. hydroxyl radicals: ˙OH) able to undergo secondary reactions. The most effective functional materials for photocatalytic applications are nano sized semiconductor oxides since it has a great potential to contribute to such environmental problems. Until now, many kinds of semiconductors have been studied as photocatalyst including TiO_2, ZnO, CdS, WO_3, etc. Most of these semiconductor photocatalysts have band gap in the ultraviolet (UV) region, i.e., equivalent to or larger than 3.2 eV (λ = 387 nm). Therefore, they promote photocatalysis upon illumination with UV radiation [1, 2].

In recent years, it has been demonstrated that semi-conducting materials mediated photocatalytic oxidation of organic compounds is a successful, convention alternative to conventional methods for the removal of organic pollutants from water [3]. The uses of ZnO as a photocatalytic degradation material for environmental pollutants have also been extensively studied, due to its nontoxic nature, low cost, and high photochemical reactivity. However, for higher photocatalytic efficiency and many practical applications, it is desirable that ZnO photocatalyst should absorb not only UV but also visible light. To absorb visible light, band gap of ZnO has to be narrowed or split into several subgaps, which can be achieved by implanting transition metal ions or by doping nitrogen [4, 5]. ZnO probably has the most abundant forms of any known material. The properties of ZnO are strongly dependent on its structure, including the morphology, aspect ratio, size, orientation, and density of crystal [6, 7]. ZnO has emerged to be more efficient catalyst as far as water detoxification is concerned because it generates H_2O_2 (hydrogen peroxide, used as a weak oxidizer, bleaching agent and disinfectant) more efficiently, it has high reaction and mineralization rates, and it has more numbers of active sites with high surface reactivity [8-11].

Heterogeneous photocatalytic materials with high efficiency and low cost was considered as one of the effective futuristic water purification methods. Once these photocatalysis materials have been developed, heterogeneous photocatalytic can be applied for high throughput systems in environment protection. Most common heterogeneous photocatalysts are transition metal oxides and semiconductors, which have unique characteristics. Unlike the metals which have a continuum of electronic states, semiconductors possess a void energy region where no energy levels are available to promote recombination of an electron and hole produced by photoactivation in the solid. The void region, which extends from the top of the filled valence band to the bottom of the vacant conduction band, is called the band gap [12]. When a photon with energy equal to or greater than the materials band gap is absorbed by the semiconductor, an electron is excited from the valence band to the conduction band, generating a positive hole in the valence band. The excited electron and hole can recombine and release the energy gained from the excitation of the electron as heat. Recombination is undesirable and leads to an inefficient photocatalyst. The ultimate goal of the process is to have a reaction between the excited electrons with an oxidant to produce a reduced product, and also a reaction between the generated holes with a reductant to produce an oxidized product. Due to the generation of positive holes and electrons, oxidation-reduction reactions take place at the surface of semiconductors. In the oxidative reaction, the positive holes react with the moisture present on the surface and produce a hydroxyl radical. Using SCs photocatalysts for the removal of organic pollutants in wastewater has attracted a lot of attention as an important issue on environmental protection.

It is known that, the photocatalytic degradation involves several steps such as adsorption-desorption, electron-hole pair production, recombination of electron pair, and chemical reaction. When the photocatalyst (PC) is irradiated with photons of energy equal to or more than band gap energy of PC, the electrons (e^-) are excited from the valence band (VB) to the conduction band (CB) with the simultaneous creation of holes (h^+) in the VB:

$$PC + h\nu \rightarrow e_{CB}^- + h_{VB}^+ \quad (1)$$

where, hν is the energy essential to transfer the electron from valence band to conduction band. The electrons generated through irradiation

*Corresponding Author
Email Address: raj_mtwu30@yahoo.co.in(R. Rajakumari)

Cite this Article as: V. Nirmala, S. Kalaiarasi, R. Rajakumari, Enhanced photocatalytic activity of undoped ZnO on methtyl orange in comparison with doped ZnO and theoretical insight on its properties, J. Nanosci. Tech. 3(4) (2017) 299–303.

could be readily trapped by O_2 absorbed on the photocatalyst surface or the dissolved O_2 to give superoxide radicals ($O_2^{\bullet -}$):

$$e_{CB}^- + O_2 \rightarrow O_2^{\bullet -} \quad (2)$$

The present work deals with the preparation of undoped and doped ZnO nanoparticles using wet chemical reaction method, characterization and application in the presence of UV radiation for photocatalytic degradation of methyl orange.

2. Experimental Methods

2.1 Sample Preparation

The undoped and transition metal ion doped ZnO nanopowder was synthesized by wet chemical reaction method. In this method, Zinc nitrate hexahydate ($Zn(NO_3)_2.6H_2O$), Sodium hydroxide (NaOH), Titanium dioxide (TiO_2), $Cu_2SO_4.5H_2O$ and $Mn(CH_3COO)_2$ of analytical grade were used as precursors. All the glass wares used in this experimental work were acid washed. The chemical reagents used were analytical reagent grade without further purification. Ultrapure water was used for all dilution and sample preparation.

To synthesize TiO_2 doped ZnO, 0.9 Mole of $Zn(NO_3)_2.6H_2O$ and 0.1 Mole of TiO_2 were dissolved in 45 ml of distilled and taken in a beaker (Solution A). This mixture is magnetically stirred (960 rpm) at room temperature in an air atmosphere. To this mixture 1 Mole of NaOH, dissolved in 5 ml of distilled water (Solution B) was added drop wise in a burette under constant stirring. This refluxing process under magnetic stirring was carried out for two hours. The resultant precipitate was sonicated in a sonicator bath for half an hour at 35 °C and it was centrifuged with distilled water and ethanol several times to remove impurities. The final precipitate was filtered and dried in an oven at 100 °C for 24 hours. The same protocol was followed to synthesize other transition metal ion (Cu^{2+} and Mn^{2+}) doped ZnO nanoparticles by substituting TiO_2 by Copper sulphate pentahydate ($Cu_2SO_4.5H_2O$), and Manganese acetate ($Mn(CH_3COO)_2$) respectively. The undoped ZnO nanoparticle was also synthesized by following the same procedure in the absence of the doping material.

3. Results and Discussion

3.1 Structural Analysis

The synthesized samples were characterized using X-ray diffraction analysis to study structural properties of the material. The XRD pattern of undoped ZnO (Fig. 1), can be indexed to hexagonal wurtzite structure of bulk ZnO. Diffraction peaks corresponding to the planes (100), (002), (101), (110), (103), and (201) are consistent with the JCPDS data of ZnO. It is observed that in the XRD patterns of doped ZnO (Fig. 2), additional peaks were present along with the characteristic peaks of ZnO, confirms the formation of nanocomposite. The sharp intense peaks in the XRD patterns indicate the crystalline nature of synthesized sample. In the XRD pattern of Mn doped ZnO, it is observed that the intensity of the characteristic peaks of ZnO is completely suppressed and the peaks due to Mn is more dominant in it, in comparison with the XRD patterns of TiO_2 and Cu. The crystallite size of undoped and doped ZnO was determined by means of an X-ray line-broadening method using the Scherer equation. The estimated size of the samples from XRD pattern ranges from 22 to 40 nm (Table 1).

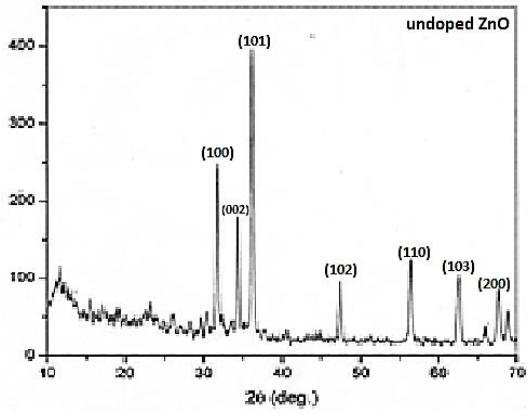

Fig. 1 XRD pattern of Undoped nano ZnO

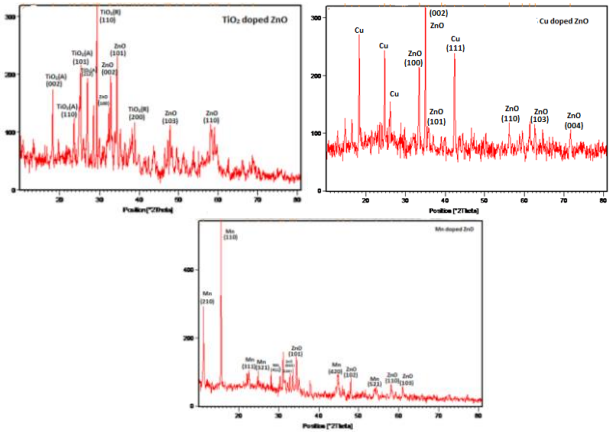

Fig. 2 XRD pattern of Transition metal ion doped nano ZnO

Table 1 Crystallite size of undoped and doped ZnO

Sample	Crystallite Size D = (0.9 λ /β cos θ) (nm)
Undoped ZnO	30
TiO_2 doped ZnO	40
Cu doped ZnO	37
Mn doped ZnO	22

3.2 Morphological Study

The surface morphology of the synthesized samples (undoped and transition metal ion doped ZnO nanopowders) was investigated using Scanning electron microscopic (SEM) technique. The SEM images of undoped ZnO (Fig. 3a) show rod-like morphology clustered together form a flower like pattern. Fig. 3b shows the SEM images of TiO_2 doped ZnO. It is observed that the SEM images show nanoflakes, in a stacked arrangement with the particle size ranging from 44 nm to 52 nm. The SEM images of Cu doped ZnO (Fig. 3c) exhibit rod-like shape. An orderly arrangement of nanoflakes with the particle size distribution ranging from 53 – 70 nm, observed in the SEM images of Mn doped ZnO (Fig. 3d).

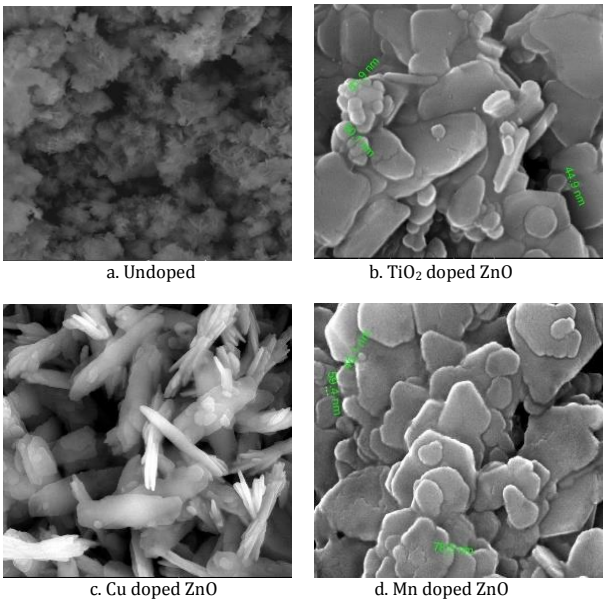

Fig. 3 SEM images of undoped and doped ZnO

3.3 Optical Properties: UV – Vis Absorption Analysis of Undoped and Doped Nano ZnO

Nanoparticles have optical properties that are sensitive to size, shape, concentration, agglomeration state, and refractive index near the nanoparticle surface, which makes UV/Vis absorption spectroscopy a valuable tool for identifying, characterizing, and studying these materials. Optical-absorption measurement is an initial step to observe the single colloid and metal-semiconductor nanocomposite behavior.

Fig. 4 gives the room temperature absorption spectra of undoped and transition metal ion doped nano ZnO. The excitonic peak of undoped and transition metal ion doped ZnO colloids is found to be blue shifted with respect to that of bulk ZnO, which could be attributed to the confinement effects. For TiO_2 doped ZnO, the surface Plasmon band lies in the 200 – 300 nm.

Cite this Article as: V. Nirmala, S. Kalaiarasi, R. Rajakumari, Enhanced photocatalytic activity of undoped ZnO on methtyl orange in comparison with doped ZnO and theoretical insight on its properties, J. Nanosci. Tech. 3(4) (2017) 299–303.

Although the conduction and valence bands of semiconductors are separated by a well-defined band gap, metal nanoclusters have close-lying bands and electrons move freely. The free electrons give rise to a SPA band in metal clusters, which depends on both the cluster size and chemical surroundings. The plasmon band of metal particles, as explained on the basis of the Mie theory, involves dipolar oscillations of the free electrons in the conduction band that occupy energy states near the Fermi level. The optical-absorption spectra of the transition metal ion doped ZnO, show a gradual shift in absorbance toward the UV region, over which an extremely weak surface plasmon resonance is superposed.

The sharpness of the absorption peak, observed from the absorption curve of both undoped and doped ZnO indicates the monodispersed nature of the nanoparticle distribution. The absorption edges observed at 232 nm (for TiO_2 doped ZnO), 231 nm (for Cu doped ZnO), 210 nm (for Mn doped ZnO) lie much below the absorption edge of bulk ZnO (388 nm). This indicates a blue shift in the spectrum.

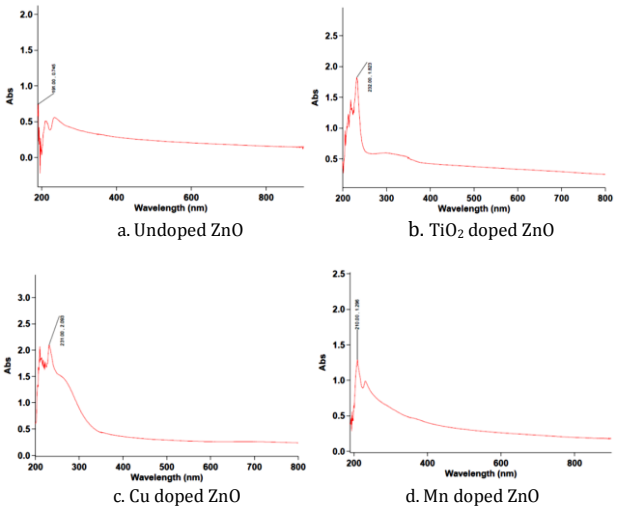

a. Undoped ZnO b. TiO_2 doped ZnO

c. Cu doped ZnO d. Mn doped ZnO

Fig. 4 UV - Vis absorption spectra of Undoped and Doped ZnO

3.4 Magnetic Properties

Transition metal (TM) doped ZnO is being highly explored, for the attainment of ferromagnetic ground state with a Curie temperature (TC) greatly exceeding room temperature, leading to a novel behaviour for the use of both charge and spin of electrons for their promising applications in spintronic devices. The coexistence of magnetic, optical properties and other heterojunction applications increase the potential of TM-doped ZnO (ZnO:TM) to be a multifunctional material. ZnO-based DMSs have been studied intensively following the theoretical prediction of room temperature ferromagnetism (RTFM) by Mn-doping in p-type ZnO or by Co doping in n-type ZnO [13-15].

The magnetic properties of transition metal ion doped ZnO was studied using Vibrating sample magnetometer (VSM) arrangement. M-H curves of doped ZnO is shown in Fig. 5. A distinct ferromagnetic curve is observed at room temperature for all three samples. Saturation magnetization, coercivity and retentivity determined from M-H curve is given in Table 2. The narrow hysteresis loop observed in the M-H curves of doped ZnO, indicate the soft magnetic nature of the samples.

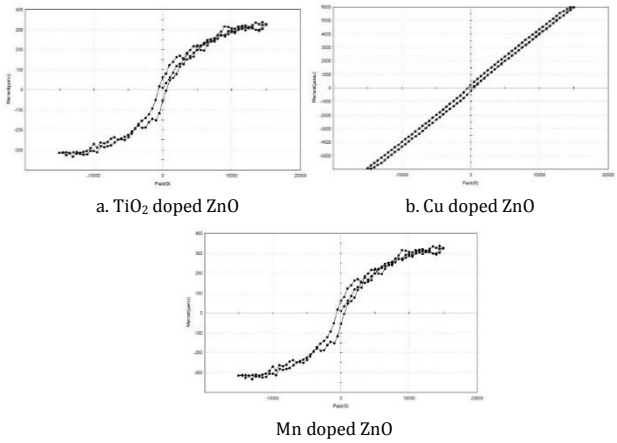

a. TiO_2 doped ZnO b. Cu doped ZnO

Mn doped ZnO

Fig. 5 M-H curves of Transition metal ion doped ZnO

Table 2 Magnetic parameters of doped ZnO, measured at room temperature

Sample Type	Magnetization (emu/g)	Coercivity (Gauss)	Retentivity (emu)	Mass susceptibility (χ) (m^3/Kg)
TiO_2 doped ZnO	$334.64X10^{-6}$	581.29	$59.424 X10^{-6}$	$0.0351 X10^{-14}$
Cu doped ZnO	$5.96 X10^{-3}$	423.01	$220.02 X10^{-6}$	$0.6260 X10^{-14}$
Mn doped ZnO	$752.06 X10^{-6}$	551.90	$61.983 X10^{-6}$	$0.0790 X10^{-14}$

The mass susceptibility (Table 2) is found to be higher for Cu doped ZnO in comparison with other dopants. It is also observed from the VSM study that, for Cu doped ZnO, the M-H curve indicate relaxed ferromagnetic effect due to decrease in the size of the particle as well as due to the effect of magnetostriction.

Thus, ferromagnetism in the transition metal ion doped ZnO nanoparticles could be considered as a result of the exchange interaction between free delocalized carriers (hole or electron) and the localized d - spins on the Ti^{4+}, Cu^{2+} and Mn^{2+}ions. Native point defects such as O vacancy and Zn interstitial are very common in ZnO and they are likely to contribute to the observed ferromagnetism in the doped ZnO nanocrystals. The ferromagnetic properties could be derived from the doping of magnetic ions, intrinsic defects, interfaces, and grain boundaries in the transition metal ion doped ZnO.

3.5 Application: Photocatalytic Degradation Activity

The photocatalytic study was performed by the degradation of aqueous methyl orange (MO). In the present study, the synthesized undoped and transition metal ion (Ti^{4+}, Cu^{2+} and Mn^{2+}) doped ZnO nanopowder were employed as photocatalysts for the degradation of methyl orange (Fig. 6). Methyl orange is an azo dye with the molecular formula $C_{14}H_{14}N_3NaO_3S$ and molecular mass is 327.34 (g/mol).

3.5.1 Irradiation Experiment

The stock solution was prepared by dissolving 0.01 g of methyl orange ($C_{14}H_{14}N_3NaO_3S$) in 100 mL of distilled water. To 10 mL of this stock solution, 0.1 g of photocatalyst (undoped ZnO and TiO_2 / Cu / Mn doped ZnO) was added. The aqueous solution was magnetically stirred for half an hour and exposed to UV light (short wavelength, 254 nm). At different time intervals, the absorption spectra were recorded.

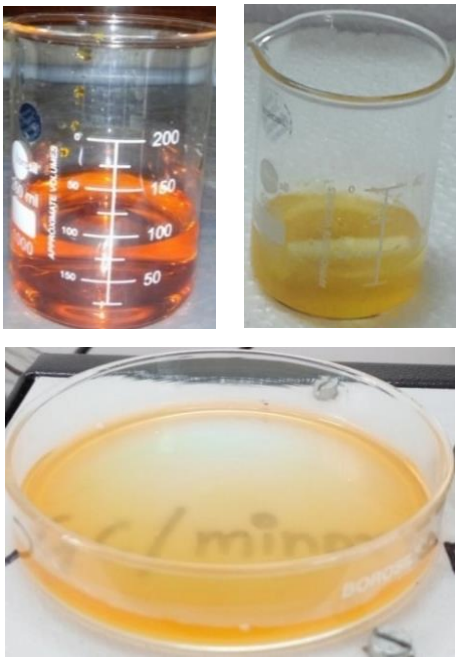

Fig. 6 Concentration of methyl orange before and after UV irradiation without and with photocatalysts (undoped and doped ZnO)

3.5.2 Degradation of Dye (MO) using Photocatalyst (Undoped and Doped ZnO)

A good catalyst should be stable under operation conditions. For this, the chemical stability of the undoped and doped ZnO photocatalysts was assessed. The photocatalytic activity of undoped and doped ZnO after prolonged exposure to UV light in aqueous solution was investigated. The optical absorption spectra were recorded and rate of degradation was observed in terms of change in intensity at λmax (462 nm) of the dye as shown in Fig. 7. It shows the optical absorption spectra of MO with

Cite this Article as: V. Nirmala, S. Kalaiarasi, R. Rajakumari, Enhanced photocatalytic activity of undoped ZnO on methtyl orange in comparison with doped ZnO and theoretical insight on its properties, J. Nanosci. Tech. 3(4) (2017) 299–303.

different photocatalyst (undoped and TiO_2/Cu/Mn doped ZnO) at different irradiation time. It is observed from the absorption spectra that the intensity of the absorption is decreasing gradually as the time increases, indicates that MO is suffering degradation during the photocatalytic reaction under UV irradiation.

It can be seen from the absorption spectra that the degradation rate of undoped ZnO is greater than (TiO_2/Cu/Mn) doped ZnO. It is observed that there is no prominent absorption peak for the dye, when undoped ZnO is added to it and also it is noted from the spectra that, as the irradiation time increased from 10 to 30 minutes, the absorption peak is completely paralyzed. The undoped ZnO completely decomposed the dye, accordingly; more photo-induced electron and holes can be produced resulting in more superoxy (super oxide radicals) species to participate photocatalytic degradation reaction. It is observed from the study that the dopants suppressed the photocatalytic activity of ZnO. Among the dopants, the degradation rate for Manganese higher than the other two dopants (TiO_2 and Cu). It is known that TiO_2 is a good photocatalyst, when it is doped with ZnO, a significant reduction in the phtocatalytic activity of ZnO is observed.

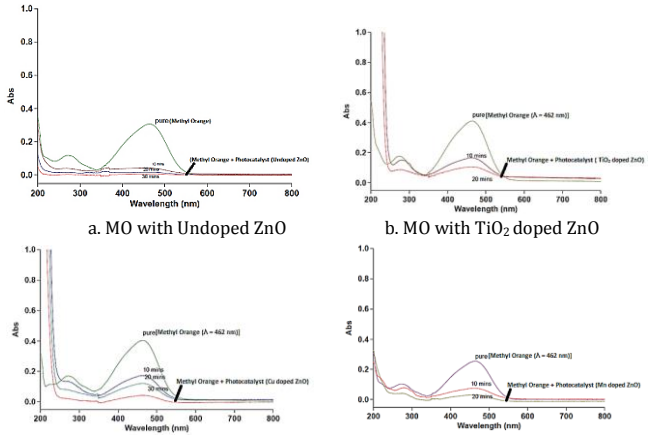

a. MO with Undoped ZnO b. MO with TiO_2 doped ZnO

c. MO with Cu doped ZnO d. MO with Mn doped ZnO

Fig. 7 Absorption spectra of MO degradations

3.6 Theoretical Investigation on the Properties of Undoped and Doped ZnO

To understand the experimental observations and to get insights on the behaviour of undoped ZnO and doped ZnO, theoretical approach been applied by taking small spherical Zn_6O_6 cluster considering it in wurtzite structure. Zn_6O_6 cluster considered in this study are the smallest representative models which contain all the atoms on the surface and also from the chemical point of view. Zn_6O_6 has equal number of active two coordinated atoms. These models would be better used to correlate the experimental observations. In this study, a theoretical analysis of undoped Zn_6O_6 and metal ion doped Zn_6O_6 cluster constructed from the optimized wurtzite structure is presented. Initially Zn_6O_6 cluster is constructed similar to the wurtzite structure and is optimized. To add the metal ion impurity a Zinc atom was randomly chosen and substituted by the impurity ion. For the undoped Zn_6O_6 cluster, the optimized structure is similar to that of the previous result. Calculations namely geometry optimization, vibrational analysis and molecular orbital calculations for undoped and doped Zn_6O_6 clusters were carried out using density functional theory. Hybrid B3LYP functional [16, 17] coupled with medium sized 6-31G* basis set has been used to optimize these clusters. There are no imaginary frequencies which confirmed that the structures are true local minima. Previous studies have shown that B3LYP provides reasonable results for small ZnO clusters [18] and also the band gap values of various metal oxides are reliably predicted [19]. All the calculations are done in Gaussian 09W [20].

The side view and top view of these undoped and doped clusters are shown in Table 3. The undoped Zn_6O_6 structure is formed by two hexagonal rings placed one above the other to form a hexagonal prism i.e., drum like structure and it is found to be most stable structure. Then it is doped with Cu^{1+}, Cu^{2+} Mn^{2+} and Ti^{4+} by removing one Zinc atom. When these ions are doped, structural changes occur and hence there is a change in bond length and bond angle and are listed in Table 4. In undoped Zn_6O_6 cluster, there are two different types of Zn-O bonds i.e., Zn-O is in the same layer and between two Zn_3O_3 rings. Also, there are two different bond angles namely Zn-O-Zn angle and O-Zn-O bond angle. In this, cluster Zn-O-Zn angle is less than the O-Zn-O bond angle and it is shown in Table 4. For undoped Zn_6O_6 there is no bond between O and Zn of atoms of Zn_3O_3 rings. But when Zinc atom is replaced by metal dopant, it is seen that new bond is formed between the dopant and oxygen atom of the adjacent Zn_3O_3. When the dopant is Ti^{4+} it is observed that the structure is totally distorted and Zn-O-Zn bond angle is broken.

Table 3 Optimised structures of undoped and transition metal ion doped Zn_6O_6 cluster

Structures	Top view	Side view
Zn_6O_6	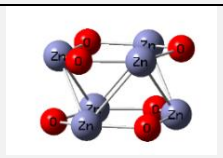	
Zn_5CuO_6 (X=Cu^{2+})	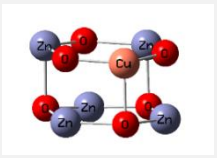	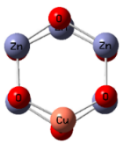
Zn_5MnO_6 (X=Mn^{2+})	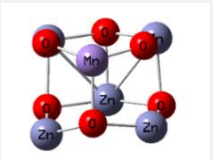	
Zn_5TiO_6 (X=Ti^{4+})	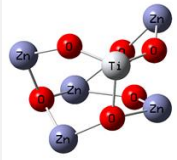	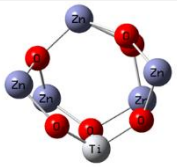

Table 4 Structural parameters of undoped and metal ion doped Zn_6O_6 cluster

Structures $Zn_{6-n}X_nO_6$ (N=0,1) (X=Cu^{2+}, Mn^{2+}, Ti^{4+})	Bond Length (in Å)			Bond Angle (in degrees)	
	Zn-O	Zn-Zn	X-O	Zn-O-Zn	O-Zn-O
Zn_6O_6	1.886	2.595	-	106.8	132.8
Zn_5CuO_6 (Cu^{2+})	1.889	2.992	1.804	115.7	124.4
Zn_5MnO_6 (Mn^{2+})	1.947	2.646	1.626	114.3	122.2
Zn_5TiO_6 (Ti^{4+})	1.885	-	1.689	Distorted	109.6

Table 5 Electronic properties of undoped and metal ion doped Zn_6O_6 cluster

Electronic Properties (in eV)	Structures $Zn_{6-n}X_nO_6$ (N=0,1) (X=Cu^{2+},Mn^{2+}, Ti^{4+})			
	Zn_6O_6	Zn_5CuO_6 (X=Cu^{2+})	Zn_5MnO_6 (X=Mn^{2+})	Zn_5TiO_6 (X=Ti^{4+})
Dipole Moment	0.0025	1.6130	3.5538	4.0435
Ionization Potential	0.24838	0.57351	0.56111	0.84174
Electron Affinity	0.11034	0.47459	0.44304	0.71651
Energy Gap	3.756	2.6916	3.2127	3.4075
Chemical Hardness	1.878	1.3458	1.6063	1.70375
chemical Potential	-4.8804	-14.2594	-13.6615	-21.20

When the metal ions Cu^{2+}, Mn^{2+} are doped in Zn_6O_6 cluster, it is observed that the distortions are caused inside the parent cluster and even extents to the breaking of the structure, when the dopant is Ti^{4+}. When there is a structural change, it induces changes in the electronic properties of the parent cluster. Hence, we have calculated the electronic properties of the modelled clusters, for both undoped and doped clusters and are correlated with the experimental observations. All the calculated electronic properties are tabulated in Table 5. The band gap for Zn_6O_6 cluster, which mimics the wurtzite structure calculated by density functional theory is ~3.7 eV, which is close to the experimentally calculated band gap value i.e ~3.3 eV [9]. The band gap of Zn_6O_6 cluster is defined as the difference between the calculated lowest unoccupied molecular orbital (LUMO) and the highest occupied molecular orbital (HOMO). The band gap shows the energy cost for an electron to jump from the HOMO to the LUMO. A large band gap correlates with high kinetic stability. The band gap energy as a function of undoped and doped clusters are shown in Fig. 8. It is observed that undoped Zn_6O_6 cluster shows larger band gap when compared with other metal ion doped Zn_6O_6 cluster. Chemical hardness, which is proportional to the band gap energy is shown in Table 2. The ionization potential and electron affinity is found to be less for undoped Zn_6O_6 cluster. Hence from all these electronic properties shown in Table 2, it is observed that undoped Zn_6O_6 is more kinetically stable rather than the metal ion doped Zn_6O_6 cluster. The dipole moment of undoped and doped Zn_6O_6

Cite this Article as: V. Nirmala, S. Kalaiarasi, R. Rajakumari, Enhanced photocatalytic activity of undoped ZnO on methtyl orange in comparison with doped ZnO and theoretical insight on its properties, J. Nanosci. Tech. 3(4) (2017) 299–303.

cluster is shown in Table 2. It shows that dipole moment is high for undoped Zn_6O_6cluster and it decreases for metal ion doped clusters. The density of states of these clusters are also shown in Fig. 9.

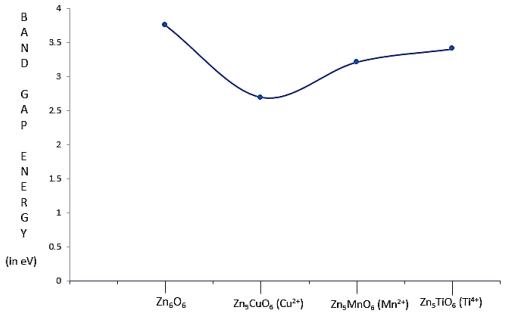

Fig. 8 Band gap energy plot of Undoped and Transition Metal ion doped Zn_6O_6 cluster

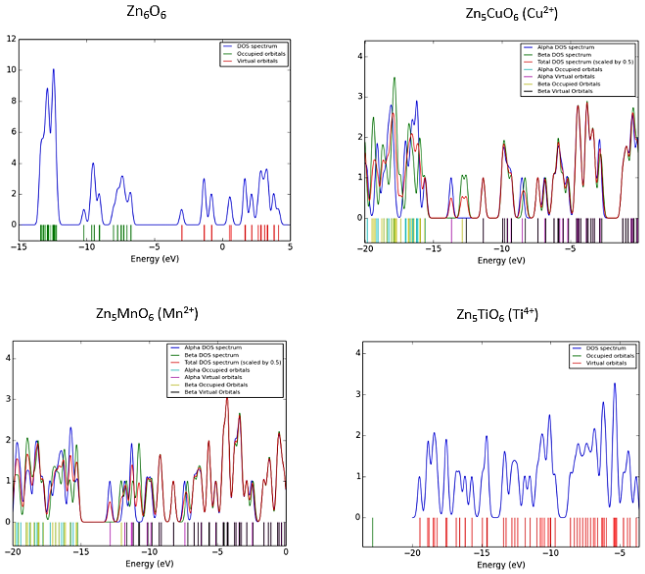

Fig. 9 Density of states of Undoped and Transition Metal ion doped Zn_6O_6 cluster

4. Conclusion

Undoped and doped ZnO nanoparticles were prepared using the wet chemical reaction method, characterized and utilized as an effective photocatalyst for the degradation methyl orange. Instrumental methods (XRD, SEM, UV– Vis) reveal and confirm the formation of nanoparticles of sizes in the range of 22 – 40 nm. The VSM measurements of Transition metal ion doped ZnO, exhibited room temperature ferromagnetism (RTFM). The exchange interactions between Ti^{4+}, Cu^{2+} and Mn^{2+} ions mediated by carriers contribute to the ferromagnetism at room temperature. The photocatalytic activity results showed that the undoped ZnO is more effective on the degradation of MO, which was attributed to their high surface area compared to doped ZnO, making them promising candidates for the treatment of organic waste-water. It is concluded that the undoped ZnO synthesized by wet chemical method has pronounced photocatalytic efficency in comparison with transition metal ion doped ZnO. To understand the experimental observation, a small undoped ZnO cluster in wurtzite cluster which mimicks bulk ZnO and is then doped with transition metal ions is theoretically constructed. Due to doping of metal ions it is observed that there is change in structures of the parent structure which leads to the changes in electronic properties. Based on the theoretical calculations it is observed that undoped Zn_6O_6 cluster is kinetically stable when compared with transition metal ion doped Zn_6O_6cluster.

Acknowledgement

The author (RR) wish to acknowledge University Grants Commission (New Delhi, India) for providing financial support in the form of Minor Research Project.

References

[1] R. Ullah, J. Dutta, Photocatalytic degradation of organic dyes with manganese-doped ZnO nanoparticles, J. Hazard. Mater. 156 (2008) 194-200.
[2] K. Byrappa, A.K. Subramani, S. Ananda, K.M. Lokanatha Rai, R. Dinesh, M. Yoshimura, Photocatalytic degradation of Rhodamine B dye using hydrothermally synthesized ZnO, Bull. Mater. Sci. 29 (2006) 433-438.
[3] N. Daneshvar, S. Aber, M.S. Seyed Dorraji, A.R. Khataee, M.H. Rasoulifard, Preparation and investigation of photocatalytic properties of ZnO nanocrystals: Effect of operational parameters and kinetic study, World Acad. Sci. Engineer. Technol. 5 (2007) 62-67.
[4] C. Wang, X. Wang, B.Q. Xua, J. Zhao, B. Mai, P. Peng, G. Sheng, J. Fu, Enhanced photocatalytic performance of nanosized coupled ZnO/SnO_2 photocatalysts for methyl orange degradation, J. Photochem. Photobiol. A: Chem. 168 (2004) 47-52.
[5] V.K. Meena, R.C. Meena, Studies on photo degradation of methyl orange in aqueous solution using immobilized dowex-11photocatalyst, J. Ind. Council Chem. 27 (2010) 180-184.
[6] M. Soltaninezhad, A. Aminifar, Study nanostructures of semiconductor zinc oxide (ZnO) as a photocatalyst for the degradation of organic pollutants, Int. J. Nano. Dimension 2 (2011) 137-145.
[7] R.Y. Hong, J.H. Li, L.L. Chen, D.Q. Liu, H.Z. Li, Y. Zheng, J. Ding, Synthesis, surface modification and photocatalytic property of ZnO nanoparticles, Powder Technol. 189 (2009) 426-432.
[8] R. Hong, T. Pan, J. Qian, H. Li, Synthesis and surface modification of ZnO nanoparticles, Chem. Engg. J. 119 (2006) 71-81.
[9] H.S. Goh, R. Adnan, M.A. Farruk, ZnO nanoflake arrays prepared via anodization and their performance in the photodegradation of methyl orange, Turk. J. Chem. 35 (2011) 375-391.
[10] R. Salama, F. Ghribi, A. Houas, C. Barthou, L. El Mir, Photocatalytic and optical properties of vanadium doped zinc oxide nanoparticles, Int. J. Nanoelect. Mater. 3 (2010) 133-142.
[11] J.J. Vora, S.K. Chauhan, K.C. Parmar, S.B. Vasava, S. Sharma, L.S. Bhutadiya, Kinetic study of application of ZnO as a photocatalyst in heterogeneous medium, J. Chem. 6 (2009) 531-536.
[12] A.M. Linsebigler, G. Lu, J.T. Yates, Photocatalysis on TiO_2 surfaces: Principles, mechanisms, and selected results, Chem. Rev. 95 (1995) 735-758.
[13] J.H. Shim, T. Hwang, S. Lee, J.H. Park, S.J. Han, Y.H. Jeong, Origin of ferromagnetism in Fe- and Cu-codoped ZnO, Appl. Phy. Lett. 86 (2005) 082503.
[14] C. Cong, L. Liao, J. Li, L. Fan, K. Zhang, Effects of temperature on the ferromagnetism of Mn-doped ZnO nanoparticles and Mn-related Raman vibration, Nanotechnol. 17 (2005) 1520-1526.
[15] L. Duan, X. Zhao, J. Liu, W. Geng, H. Xie, S. Chen, Structural, thermal and magnetic investigations of heavily Mn-doped ZnO nanoparticles, J. Magn. Magn. Mater. 323 (2011) 2374-2379.
[16] A.D. Becke, Density-functional thermochemistry. III. The role of exact exchange, J. Chem. Phys. 98 (1993) 5648-5652.
[17] C. Lee, W. Yang, R.G. Parr, Development of the Colle-Salvetti correlation-energy formula into a functional of the electron density, Phys. Rev. B 37 (1988) 785-789.
[18] J.M. Matxain, J.E. Fowler, J.M. Ugalde, Small clusters of II-VI materials: Zn_iO_i, i = 1–9, Phys. Rev. A 62 (2000) 053201-053211.
[19] J. Muscat, A. Wander, N.M. Harrison, On the prediction of band gaps from hybrid functional theory, Chem. Phys. Lett. 342 (2001) 397-401.
[20] M.J. Frisch, G.W. Trucks, H.B. Schlegel, G.E. Scuseria, M.A. Robb, Electronic Supplementary information polymorphic and mechanochromic luminescence modulation in the highly emissive dicyanodistyrylbenzene crystal: Secondary bonding interaction in molecular stacking assembly, Gaussian 09, Revision A.02, Gaussian, Inc., Wallingford CT, 2009.